

Cure Kinetics and Morphology of Natural Rubber Reinforced by the *In Situ* Polymerization of Zinc Dimethacrylate

Yijing Nie, Guangsu Huang, Liangliang Qu, Peng Zhang, Gengsheng Weng, Jinrong Wu

State Key Laboratory of Polymer Materials Engineering, College of Polymer Science and Engineering, Sichuan University, Chengdu 610065, People's Republic of China

Received 2 January 2009; accepted 11 May 2009

DOI 10.1002/app.31045

Published online 27 August 2009 in Wiley InterScience (www.interscience.wiley.com).

ABSTRACT: Peroxide-cured natural rubber (NR) reinforced by zinc dimethacrylate (ZDMA) was prepared. The cocrosslinking action of ZDMA and the formation and evolution of the phase morphology induced by ZDMA during the curing process were systematically investigated. A curemeter and a differential scanning calorimeter were used to investigate the cure kinetics, and the kinetic parameters and the apparent activation energy were obtained. The phase morphology of the composites obtained from transmission electron microscopy revealed

that separated nanophases of poly(zinc dimethacrylate) (PZDMA) existed in the rubber matrix. Covalent crosslinking, physical adsorption, and ionic crosslinking simultaneously existed in the composites, and they were determined with an equilibrium swelling method. On the basis of this, new microstructure models of NR/ZDMA composites and ionic crosslinking were put forward. © 2009 Wiley Periodicals, Inc. *J Appl Polym Sci* 115: 99–106, 2010

Key words: curing of polymers; phase behavior; rubber

INTRODUCTION

Compared with sulfur-cured natural rubber (NR), peroxide-cured NR has better resistance to thermooxidative aging and thermal stability, whereas the mechanical properties are slightly poorer. Therefore, some coagents need to be used to increase the crosslinking density and form a complex crosslinking network to improve the mechanical properties of peroxide-cured NR.¹ Among them, the most common coagents are chemicals with multifunctional groups, including alkyl methyl acrylate. New coagents of metal salts of methacrylic acids, especially zinc dimethacrylate (ZDMA), have been used to cure hydrogenated nitrile-butadiene rubber (HNBR) to improve the tear strength, abrasion resistance, and high-temperature performance.² Some comparisons of rubbers prepared from the coagents with those reinforced by conventional fillers such as carbon black and silica have indicated that the former have higher moduli at low extension.³ Many

researchers have investigated different kinds of rubbers reinforced by metal salts of methacrylic acids, such as NR, butadiene rubber, ethylene-propylenediene monomer, nitrile-butadiene rubber, and poly(α -octylene-co-ethylene) elastomer.^{1,3–12} They have found that ZDMA can polymerize in the rubber matrix to form nanodispersion phases acting as nanometer filling particles or to graft onto NR chains and thus enhance the crosslinking network. However, a well-accepted theory of the reinforcing mechanism has not been reached. Because the study of the cure kinetics and phase morphology of composites is the basis of determining the reinforcing mechanism in essence, many studies have been undertaken to examine the curing process and the microstructure of rubber/ZDMA composites. Lu et al.¹² found that the polymerization of ZDMA took place in advance of the crosslinking reaction of rubber with an infrared spectroscopy method, whereas Ikeda et al.¹¹ used dynamic mechanical analysis and surface tension to analyze the phase separation during curing and the copolymerization behaviors of ZDMA and 2-(*N*-ethyl perfluoro-octane sulfonamido)ethyl acrylate in HNBR. However, few have investigated the cure kinetics as well as the kinetic parameters, which are necessary to understand the complicated curing process. On the other hand, the phase morphology of composites has also attracted the attention of researchers. Nomura et al.¹³ first found nanodispersion phases [poly(zinc

Correspondence to: G. Huang (guangsu-huang@hotmail.com).

Contract grant sponsor: National Natural Science Foundation of China; contract grant number: 50673059.

Contract grant sponsor: National Basic Research Program of China; contract grant number: 2007CB714701.

dimethacrylate) (PZDMA) aggregations] in HNBR/ZDMA composites by transmission electron microscopy (TEM). Both Yuan et al.¹⁴ and Dontsov et al.,¹⁵ using small-angle X-ray scattering measurements, pointed out that a random distribution of fine particles of about 20 nm existed in vulcanizates. Moreover, a microstructure model for rubbers reinforced by ZDMA was put forward by Lu et al.⁹ However, it is a pity that many of the works on morphology are not analyzed for a thermodynamic mechanism, which generally controls the formation of the phase morphology. Besides, ionic crosslinking is supposed to play an important role in the reinforcement of rubber,¹⁰ but its structure and formation mechanism are still obscure. Therefore, intensive studies on the microstructure of NR/ZDMA composites are still needed.

In the work, curing curves, differential scanning calorimetry (DSC), the equilibrium swelling method, and TEM have been applied to study the cure kinetics and phase morphology of peroxide-cured NR reinforced by ZDMA. The results show that ZDMA can polymerize and graft onto the rubber chains to largely improve the crosslinking density of NR, and the formation and the evolution of the separated nanodispersions of PZDMA in NR are controlled by thermodynamics due to the crosslinking reaction of NR and the increasing molecular weight of PZDMA. Besides, the microstructure of the ionic crosslinking derived from the electrostatic interaction of ion pairs in PZDMA molecules has also been studied further. Finally, new structure models of the composites and the ionic crosslinking are put forward.

EXPERIMENTAL

Materials

NR (CSR-10) was supplied by Mengwang Rubber Corp. (Yulan, People's Republic of China). ZDMA was purchased from Xian Organic Chemical Technology Plant (Shanxi, People's Republic of China). Dicumyl peroxide was produced by Chengdu Kelong Chemical Technology Plant (Sichuan, People's Republic of China).

Preparation of the samples

NR was plasticated on a laboratory two-roll mill at room temperature. Then, ZDMA and dicumyl peroxide were added. After mixing, the compound was cured at 155°C in an electrically heated hydraulic press for the optimal cure time (i.e., the time to achieve to 90% of the cure), which was derived from curing curves.

Instruments and characterization

The curing process at 155°C was analyzed with a curemeter produced by Beijing Youshen Electronic Apparatus Factory (Beijing, People's Republic of China). The cure kinetics was also measured with a differential scanning calorimeter (DSC 204, Netzsch Co., Selb, Germany) at different heating rates (2, 5, 10, 15, and 20°C/min). The weights of the samples were in the range of 10–15 mg.

The crosslinking density was determined from equilibrium swelling measurements on the basis of the Flory–Rehner equation:¹⁶

$$- [Ln(1 - \Phi_r) + \Phi_r + \chi\Phi_r^2] = V_0 n \left[\Phi_r^{1/3} - \frac{\Phi_r}{2} \right] \quad (1)$$

where Φ_r is the volume fraction of the polymer in the swollen mass, V_0 is the molar volume of the solvent (106.2 cm³ for toluene), n is the number of active network chain segments per unit of volume (crosslinking density), and χ is the Flory–Huggins polymer–solvent interaction term. The value of χ for toluene is 0.393.¹⁷ The value of Φ_r was attained according to the method used by Bala et al.¹⁸

$$\Phi_r = \frac{w_2/\rho_2}{w_2/\rho_2 + (w_1 - w_2)/\rho_1} \quad (2)$$

where w_1 and w_2 are the weights of the swollen and deswollen samples, respectively, and ρ_1 and ρ_2 are the densities of the solvent and polymer, respectively.

Samples were swollen in toluene at room temperature for 7 days. Subsequently, w_1 was determined after the solvent was gently wiped off the sample surface with filter paper, and w_2 was determined after drying at 80°C until a constant weight was achieved. In this way, the whole volume fraction of the polymer and the crosslinking density could be calculated with eqs. (1) and (2). The measured crosslinking density contained the covalent crosslinking, the crosslinking caused by physical adsorption, and the ionic crosslinking. To destroy the ionic crosslinking, samples were swollen in a toluene/hydrochloric acid/ethanol mixed solvent for 3 days and then swollen in toluene for 7 days. The residual crosslinking density (the covalent crosslinking and the crosslinking caused by physical adsorption) could be obtained. The ionic crosslinking density could be calculated by subtraction of the residual crosslinking density from the whole crosslinking density.

The phase morphology of the samples was analyzed with a transmission electron microscope (JEM 2010, JEOL Co., Tokyo, Japan) under an acceleration voltage of 200 kV. The specimens for TEM observations were prepared with a Leica (Wetzlar, Germany) ultramicrotome under cryogenic conditions with a diamond knife.

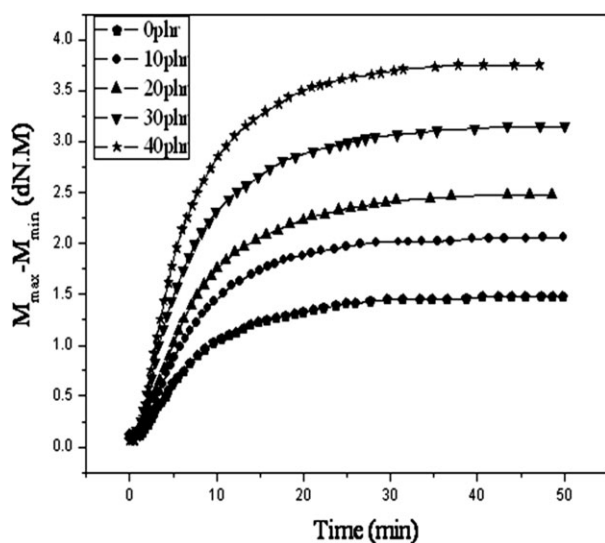


Figure 1 Curing curves for different percentages of ZDMA.

RESULTS AND DISCUSSION

Cure kinetics

Among all the factors determining the rubber properties, the formation approach and the structure of the crosslinking network are the most significant. In general, curemeters and DSC are most popular for studying the curing process because of their simple operation and reliable results.

The curing curves are shown in Figure 1. In addition, the maximum torque (M_{\max}) values, the minimum torque (M_{\min}) values, and the difference between them ($M_{\max} - M_{\min}$) are summarized in Table I. As the ZDMA content increases, $M_{\max} - M_{\min}$ increases, and this is related to the crosslinking density.¹⁷ This means that the addition of ZDMA enhances the crosslinking efficiency and the crosslinking density of NR composites. Further evidence of enhanced crosslinking in the presence of ZDMA was attained by DSC, as shown in Figure 2 and Table II. The total heat liberated during the entire curing reaction (ΔH_c) under dynamic condition increases with increasing ZDMA content. Undoubtedly, the increased heat of vulcanization should be attributed to a higher degree of crosslinking during curing in the presence of ZDMA.

When a curemeter is used to study the cure kinetics, the conversion (α) is defined as follows:¹⁹

$$\alpha = \frac{M_t - M_0}{M_{\max} - M_0} \quad (3)$$

where M_0 and M_t are the torque values at time zero and at curing time t , respectively.

Then, the relationship between the rate of conversion and the conversion can be attained, as shown in Figure 3. It is well known that chemical reactions can be divided into simple reactions and autocatalytic reactions. In a simple reaction, the maximum rate of curing occurs at the beginning, whereas in an autocatalytic reaction, the maximum rate of curing happens at a conversion degree other than zero because it is promoted by the products of the reaction.²⁰ In an autocatalytic reaction, the basic rate equation is given by²¹

$$\frac{d\alpha}{dt} = K(T)\alpha^m(1 - \alpha)^n \quad (4)$$

where $d\alpha/dt$ is the cure rate, t is the time, m and n are the orders of reaction, and $K(T)$ is the temperature-dependent reaction rate constant.

Figure 3 shows that the maximum rate of curing happens at a conversion degree of about 0.15–0.3, so the curing processes of neat NR and NR/ZDMA composites all follow the autocatalytic reaction model, and eq. (4) was chosen as the cure kinetics equation for neat NR and NR/ZDMA composites. The kinetic parameters were obtained by linear multiple regression analysis of the experimental data with Origin 7.0 computer software. The results are listed in Table I.

Moreover, many methods^{22–24} based on DSC have been employed to analyze the apparent activation energy (E_a) of the curing reaction. In this work, the Kissinger method²³ and the Ozawa method²⁴ were chosen to calculate E_a with the following equations:

$$\text{Kissinger method: } E_a = -R \frac{d \ln(\beta/T_{\max}^2)}{d(1/T_{\max})} \quad (5)$$

$$\text{Ozawa method: } E_a = -R \frac{d \ln \beta}{d(1/T_{\max})} \quad (6)$$

TABLE I
Kinetic Parameters and Curing Characteristics Obtained from Curemeter Testing

	K	n	m	M_{\max}	M_{\min}	$M_{\max} - M_{\min}$
NR	0.23	1.51	0.26	1.48	0.06	1.42
NR/10 phr ZDMA	0.36	1.75	0.54	2.06	0.08	1.98
NR/20 phr ZDMA	0.34	1.65	0.56	2.48	0.10	2.38
NR/30 phr ZDMA	0.36	1.78	0.44	3.15	0.13	3.02
NR/40 phr ZDMA	0.44	1.85	0.47	3.75	0.15	3.60

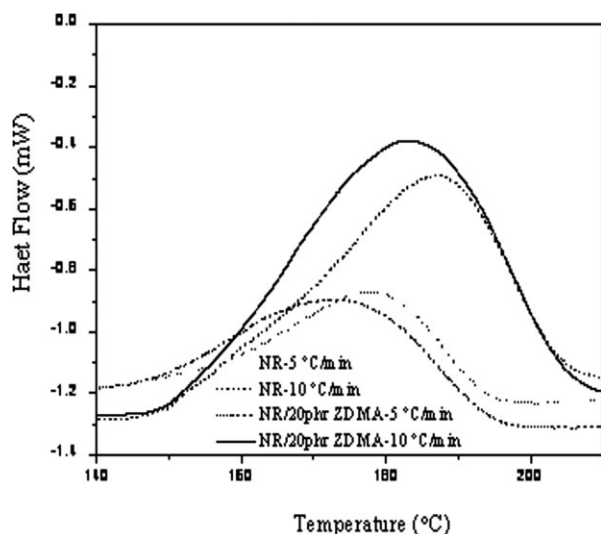


Figure 2 Typical dynamic DSC curves.

where β is the heating rate, T_{\max} is the temperature of the maximum rate of conversion, and R is the gas constant.

By drawing plots (Fig. 4) according to eqs. (5) and (6) and fitting them with a linear function, we calculated E_a from the slopes of these plots (Table II).

Table I shows that when NR is filled with ZDMA, the kinetic parameters change a lot. The values of K of filled NR are larger than those of pure NR, and this suggests that ZDMA affects and accelerates the curing reaction. In addition, the values of n and m also rise in comparison with those of pure NR, and this indicates that the reaction order changes; that is, ZDMA has taken part in the curing reaction of NR, causing a change in the crosslinking reaction mechanism in the curing system. Table II shows that the E_a value of the curing of pure NR is greater than that of NR filled with 20 phr ZDMA. At the same time,

TABLE II
 E_a Calculated from Dynamic DSC

Sample	β (°C/min)	T_{\max} (°C)	ΔH_c (J/g)	E_a (kJ/mol)	
				Kissinger	Ozawa
NR	2	167.3	8.65	133.3	140.8
	5	177.9	11.72		
	10	186.9	10.41		
	15	191.6	11.84		
	20	195.2	11.38		
NR/20 phr ZDMA	2	161.5	13.15	121.1	128.5
	5	172.7	12.36		
	10	183.5	12.33		
	15	185.8	17.74		
	20	191.9	22.47		
ZDMA	2	157.7	—	109.6	115.6
	5	165.3	—		
	10	174.2	—		
	15	183.9	—		
	20	188.9	—		

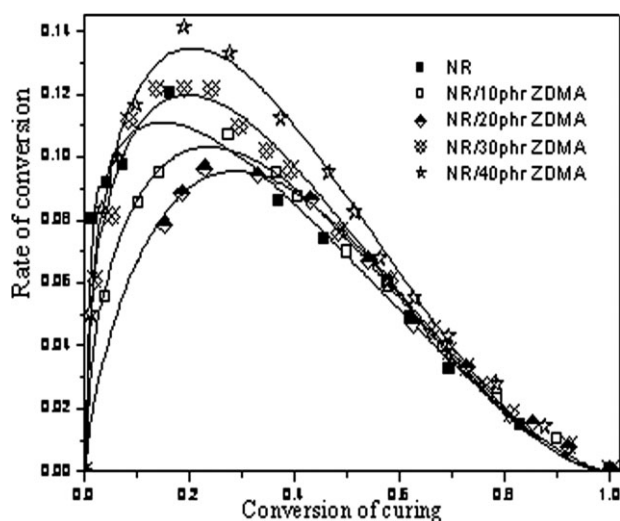


Figure 3 Rate of conversion as a function of the curing conversion of NR and NR/ZDMA composites. The solid line is the theoretical curve, and the dots represent experimental data.

NR filled with 20 phr ZDMA exhibits an obvious decrease in T_{\max} . These results are in accord with the increment of the values of K , confirming the significant effect of ZDMA on the vulcanization of NR. To validate further the impact of ZDMA on the curing of NR, DSC testing of solid-state bulk polymerization of ZDMA was also carried out, and this showed lower T_{\max} and E_a values versus those of neat NR and NR/ZDMA composites (Table II).

Therefore, all these variations can be attributed to the fact that several reactions exist in the meantime in the curing system. Peroxide radicals abstract hydrogen from methylene of molecular chains of NR, giving birth to rubber radicals. When two rubber radicals meet, a crosslinking bond is then formed. Simultaneously, ZDMA contained in the system can undergo polymerization initiated by peroxide radicals; this E_a value is lower than the E_a value of the crosslinking of neat rubber (Table II), and this results in a decrease in the whole E_a value in the curing process of NR/ZDMA composites. On the other hand, because of the presence of double bonds in the rubber, PZDMA radicals can also react with NR radicals, forming NR-graft-PZDMA. Moreover, when two PZDMA radicals meet or one PZDMA radical abstracts hydrogen from a rubber chain, a free (ungrafted) PZDMA molecule can also appear. Therefore, NR radicals inversely can also initiate ZDMA to polymerize, producing grafted PZDMA with another approach.

Phase morphology and its model

According to the analysis of the cure kinetics, at least two special products of the rubber

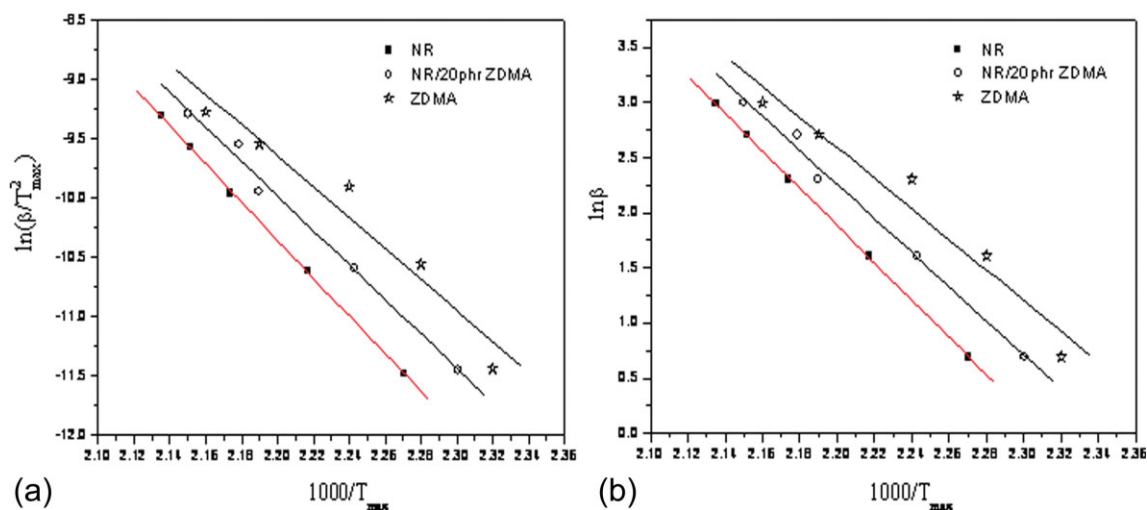


Figure 4 Dynamic DSC for calculating E_a by (a) the Kissinger equation and (b) the Ozawa equation. [Color figure can be viewed in the online issue, which is available at www.interscience.wiley.com.]

vulcanization, PZDMA and NR-*graft*-PZDMA, exist in the composites. Furthermore, the great improvement in the crosslinking density (Fig. 1) may come from NR-*graft*-PZDMA and PZDMA. To reveal the essential nature of the crosslinking action of PZDMA, the phase morphology of the composites and its evolution during curing are the matters of the most concern. The TEM images shown in Figure 5, in which the dark phase is the phase of PZDMA and the bright phase represents the phase of NR, clearly indicate that the PZDMA phases disperse in NR with a diameter of about 10–20 nm. When the crosslinking of rubber and the polymerization reaction of ZDMA happen, the morphology will be governed by the Gibbs mixing free energy, and a phase transition is preferred to develop toward the direction in which the Gibbs free energy (G)

becomes smaller.²⁵ During the curing reaction, the polymerization of ZDMA occurs, and the molecular weight of PZDMA increases. When the increasing molecular weight of PZDMA reaches a critical condition, phase separation will happen, resulting in two separated phases.²⁶

Guo²⁷ set an equation to describe G in a multi-component system:

$$G = \sum n_i \mu_i + \sum A_i \gamma_{ij} \quad (7)$$

where n_i is the molar number of component i , μ_i is the chemical potential of component i , γ_{ij} is the interfacial energy between two components (i and j), and A_i is the surface area of component i .

For a polymer blend, the value of $\sum n_i \mu_i$ is fixed, so the phase morphology is dominated by the value

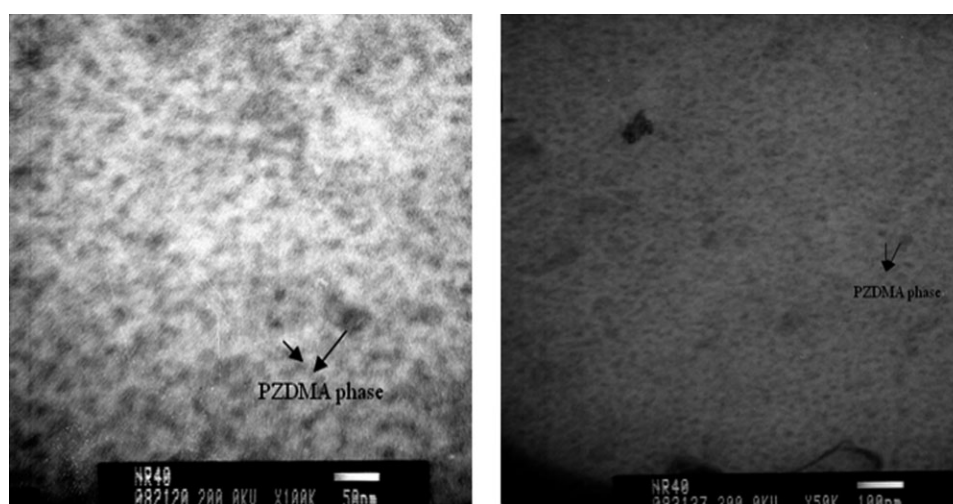


Figure 5 TEM images of NR filled with 40 phr ZDMA: (a) 50 and (b) 100 nm.

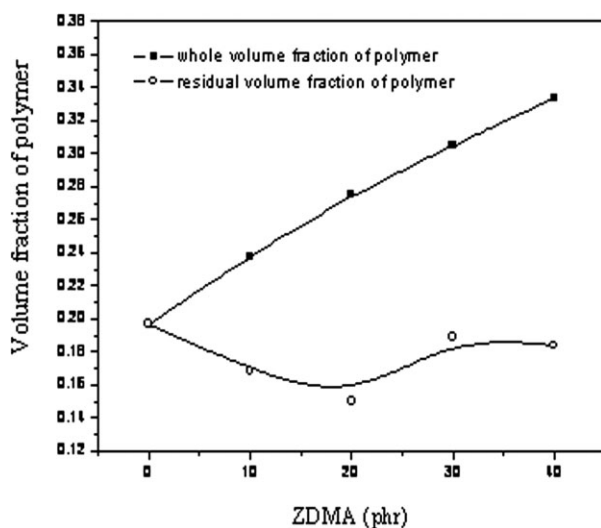


Figure 6 Volume fraction of the polymer as a function of the loading amount of ZDMA.

of $\sum A_i \gamma_{ij}$. In NR/ZDMA composites, three components—NR, NR-graft-PZDMA, and PZDMA—exist. When NR-graft-PZDMA is in the interface of NR and PZDMA, the value of γ_{ij} will decrease, and this will result in a thermodynamically stable state of the system. Thus, NR-graft-PZDMA is inclined to exist in the interface of NR and PZDMA. However, this discussion is based on an ideal situation. During curing, the viscosity of the rubber compound increases because of the crosslinking of NR and polymerization of ZDMA; thus, the diffusion capacity of the rubber chains, ZDMA, and chains of PZDMA decreases. When the viscosity increases to a degree at which the diffusion of polymer chains and monomers is limited, NR-graft-PZDMA will hardly enter

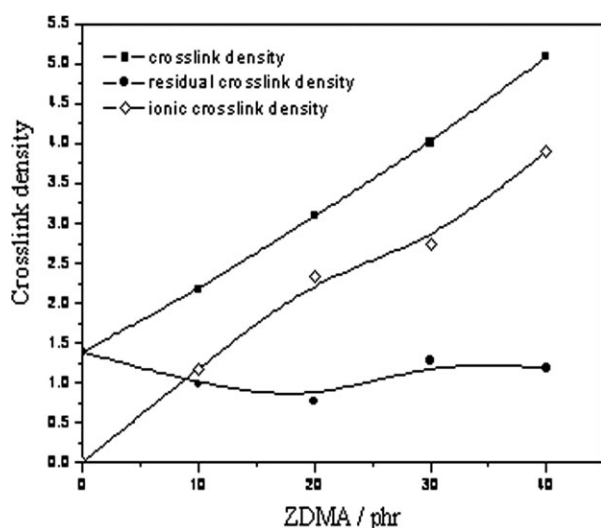


Figure 7 Three kinds of crosslink densities as a function of the loading amount of ZDMA.

TABLE III
Mechanical Properties

	NR/ZDMA				
	NR	10 phr	20 phr	30 phr	40 phr
Tensile strength (MPa)	6.6	12.4	17.9	19.0	20.2
Elongation at break (%)	510	306	266	241	230
Hardness	39	49	57	67	79

the interface of NR and PZDMA. Therefore, PZDMA can also independently act with rubber in aggregation forms by physical adsorption.

It is significant to understand the aggregation structure of the NR/ZDMA composites and its evolution, and ionic interaction is the foundation for constructing the aggregation. Because of the large numbers of ion pairs in PZDMA molecules and the strong electrostatic interaction between ion pairs, aggregates consisting of several pairs can be formed, and they are called multiplets,²⁸ restricting the mobility of adjacent polymer chains. Therefore, the principal chains of PZDMA are dominated by the multiplets, and this makes the glass-transition temperature of PZDMA rise above 300°C.⁹ Besides, some of the NR chains near PZDMA and in NR-graft-PZDMA can also be restricted by the adjacent multiplets, and these multiplets in the grafted polymer and homopolymer will act as a new kind of crosslinking action, namely, ionic crosslinking.

Because the ionic crosslinking derived from the electrostatic interaction between the ion pairs can be shielded and destroyed by chloride ions, hydrogen ions, and ethanol molecules,^{28,29} the ionic crosslinking density can be determined by subtraction of the residual crosslinking density from the whole crosslinking density measured by swelling only in

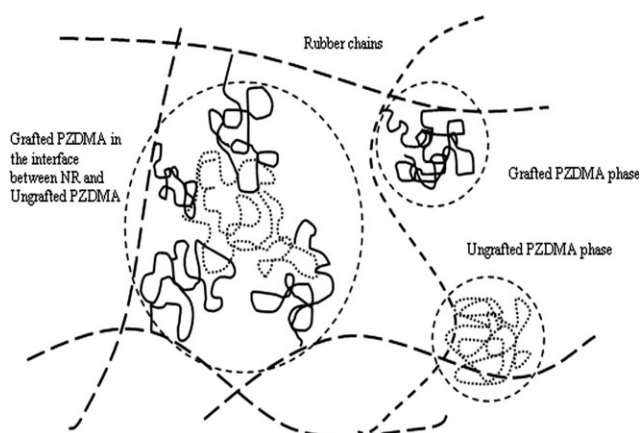


Figure 8 Microstructure model of NR/ZDMA composites.

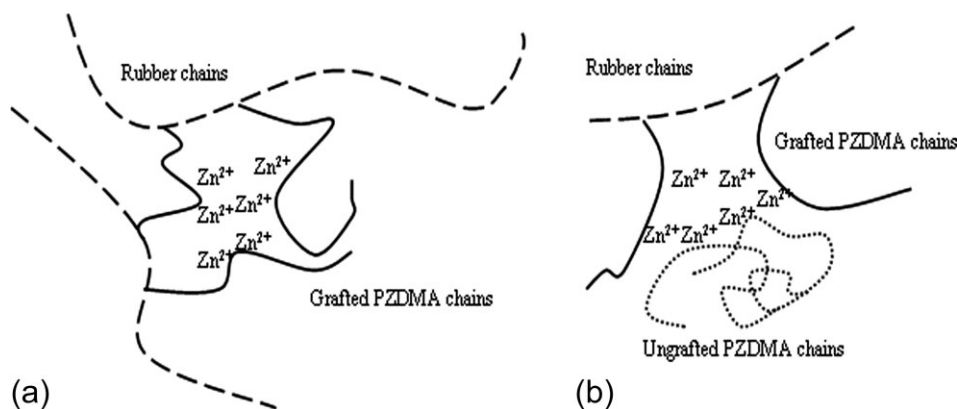


Figure 9 Microstructure of the ionic crosslinks (multiplets) formed (a) in grafted PZDMA and (b) between grafted PZDMA and ungrafted PZDMA.

toluene. Figure 6 displays the two kinds of volume fractions of the polymer, and Figure 7 shows the crosslinking densities of the three kinds of crosslinking, indicating that the whole crosslinking density and the ionic crosslinking density increase with the content of ZDMA, whereas the covalent crosslinking density changes little. Without a doubt, the ionic crosslinking induced by PZDMA makes the crosslinking network more complex and stronger, largely improving the mechanical properties of NR, as listed in Table III. A further and detailed investigation of the mechanical properties and reinforcement mechanism of NR/ZDMA composites will be discussed in a future article.³⁰

On the basis of this study, we put forward a microstructure model of NR/ZDMA composites (Fig. 8). Two phases, an NR phase and a PZDMA phase, exist. The morphology of ionic crosslinking has two forms, as shown in Figure 9. First, ionic crosslinking forms in the grafted PZDMA chains near NR; second, ionic crosslinking also forms between the grafted PZDMA chains near NR and the ungrafted PZDMA chains.

CONCLUSIONS

The increases in the torque values and the total heat of vulcanization indicate that the addition of ZDMA enhances the crosslinking density of NR/ZDMA composites. The curing reaction of NR/ZDMA composites possesses the characteristics of an autocatalytic reaction. E_a decreases when ZDMA is added. All these changes can be attributed to the coexistence of multiple crosslinking reactions in NR/ZDMA composites at elevated temperatures.

Three components—NR, NR-*graft*-PZDMA, and PZDMA—exist in NR/ZDMA composites. Because of the thermodynamic effect, NR-*graft*-PZDMA likely exists in the interface of NR and PZDMA. However, the aggregation of PZDMA, independently interact-

ing with rubber chains by physical adsorption, is also reasonable because of the increase in the viscosity during the curing reaction. Much ionic crosslinking derives from a mass of ion pairs in PZDMA chains. Finally, new structure models of NR/ZDMA composites and ionic crosslinking have been put forward to describe the fine structure of PZDMA and the ionic crosslinking in NR (as shown in Figs. 8 and 9).

References

1. Costin, R.; Nagel, W.; Ekwall, R. *Rubber Chem Technol* 1991, 64, 152.
2. Touchet, P.; Rodriguez, G.; Gatza, P. E.; Butler, D. P.; Crawford, D.; Teets, A. R.; Fener, H. O.; Flanagan, D. P. U.S. Pat. 4,843,114 (1989).
3. Roland, C. M. U.S. Pat. 4,720,526 (1988).
4. Costin, R.; Ekwall, R.; Nagel, W. *Rubber World* 1992, 27, 204.
5. Klingender, R. C.; Oyama, M.; Satio, Y. *Rubber World* 1990, 26, 202.
6. Medalia, A. I.; Alesi, A. L.; Mead, J. L. *Rubber Chem Technol* 1992, 65, 154.
7. Saito, Y.; Nishimura, K.; Asada, M.; Toyoda, A. *Jpn Rubber Soc* 1994, 67, 867.
8. Lu, Y. L.; Liu, L.; Yang, C.; Tian, M.; Zhang, L. Q. *Eur Polym J* 2005, 41, 577.
9. Lu, Y. L.; Liu, L.; Tian, M.; Geng, H. P.; Zhang, L. Q. *Eur Polym J* 2005, 41, 589.
10. Peng, Z.; Liang, X.; Zhang, Y.; Zhang, Y. *J Appl Polym Sci* 2002, 84, 1339.
11. Ikeda, T.; Yamada, B.; Tsuji, M.; Sakurai, S. *Polym Int* 1999, 48, 446.
12. Lu, Y.; Liu, L.; Shen, D.; Yang, C.; Zhang, L. *Polym Int* 2004, 53, 802.
13. Nomura, A.; Takano, J.; Toyoda, A.; Saito, T. *Jpn Rubber Soc* 1993, 66, 830.
14. Yuan, X.; Zhang, Y.; Peng, Z.; Zhang, Y. *J Appl Polym Sci* 2002, 84, 1403.
15. Dontsov, A.; De Candia, F.; Amelino, L. *J Appl Polym Sci* 1972, 16, 505.
16. Flory, P. J. *Principles of Polymer Chemistry*; Cornell University Press: Ithaca, NY, 1953; p 576.
17. Arroyo, M.; López-Manchado, M. A.; Herrero, B. *Polymer* 2003, 44, 2447.

18. Bala, P.; Samantaray, B. K.; Srivastava, S. K.; Nando, G. B. *J Appl Polym Sci* 2004, 92, 3583.
19. Kader, M. A.; Nah, C. *Polymer* 2004, 45, 2237.
20. López-Manchado, M. A.; Arroyo, M.; Herrero, B.; Biagiotti, J. *J Appl Polym Sci* 2003, 89, 1.
21. Piloyan, G. O.; Ryabchikov, I. D.; Novikova, O. S. *Nature* 1966, 212, 1229.
22. Borchardt, H. J.; Daniel, F. Y. *J Am Chem Soc* 1956, 79, 41.
23. Kissinger, H. E. *Anal Chem* 1957, 29, 1702.
24. Ozawa, T. *Bull Chem Soc Jpn* 1965, 38, 1881.
25. Zhou, L. *Physical Chemistry*; Science: Beijing, 2002; p 32.
26. He, M. J.; Chen, W. X.; Dong, X. X. *Polymer Physics*; Fudan University Press: Shanghai, 1990; p 141.
27. Yin, J. H.; Mo, Z. S. *Modern Polymer Physics*; Science: Beijing, 2001; p 276.
28. Eisenberg, A.; Hird, B.; Moore, R. B. *Macromolecules* 1990, 23, 4098.
29. Smith, P.; Eisenberg, A. *J Polym Sci Part B: Polym Phys* 1988, 26, 569.
30. Nie, Y. J.; Huang, G. S.; Qu, L. L.; Zhang, P.; Weng, G. S.; Wu, J. R. *J Appl Polym Sci*, to appear.